

# Lattice Study of Scalar Mesons and Exotic Hadrons

Atsushi Nakamura  
in collaboration with

Scalar Collaboration (T. Kunihiro, S. Muroya, C. Nonaka, M. Sekiguchi and A. Wada)  
and T. Saito  
*RIISE, Hiroshima University, Higashi-Hiroshima, 739-8521, Japan*

We report two lattice QCD simulation projects relating to multi-quark states: 1) full QCD simulations of scalar mesons,  $\sigma$  and  $\kappa$  using Wilson fermions, and 2) quench calculation of diquark force using Polyakov line correlations.

We observe a low sigma mass,  $m_\pi < m_\sigma \leq m_\rho$ , for which the disconnected diagram plays an important role. For the kappa meson, we obtain higher mass than the experimental value, *i.e.*  $m_\kappa \sim 2m_{K^*}$ .

Then, we describe formula to obtain the  $q - q$  force, and show results at finite temperature. An approach is proposed to study the force between two quarks in the confinement region.

PACS numbers:

## I. INTRODUCTION

This symposium focuses a very ambitious topics, *i.e.*, “multiquark hadrons”. A question why hadrons are a bound state of only three quarks or quark-antiquark system originated from the early days of the quark model, and now after the discovery of the penta-quarks[1], we should go a step further, *i.e.*, what kind of multi-quark systems are available in QCD and what kind of dynamics works behind.

In this workshop, Prof. Jaffe gave a beautiful lecture, where he described successfully the penta-quarks together with other multiplets using the di-quark degrees of freedom. Quark-quark system is color anti-triplet (anti-symmetric) or sextet (symmetric),

$$\begin{aligned} 3 \times 3 &= 3^* + 6 \\ \square \times \square &= \square + \square \end{aligned} \tag{1}$$

We may anticipate that, in the color anti-triplet channel, the quark-quark interaction is attractive and strong based on the perturbation [4] and the instanton induced model [5]. The penta-quark state,  $\Theta^+$ , may be a bound state of  $(ud)(ud)\bar{s}$ , where  $(ud)$  stands for highly correlated  $u$  and  $d$  quark pairs.[6] Di-quark states play an important role not only in multi-quark states, but also in high energy reactions and color superconductivity at high density.[3] There has been, however, no lattice calculation to investigate the force between two quarks. In the second part of this paper, we report our lattice simulation project of the  $q - q$  potential.

Even the scalar particle,  $\sigma$ , may be included in this framework. In Ref.[7], Alford and Jaffe calculated  $\pi - \pi$  scattering amplitude in the quench approximation by Lüscher formula with neglecting diagrams (A) and (G) in Fig.2, and found an evidence of the bound state, and proposed a new picture of the scalar mesons as a  $(\bar{q}\bar{q})(qq)$  state.

In this paper, we report our approaches to the sigma meson and di-quark force.

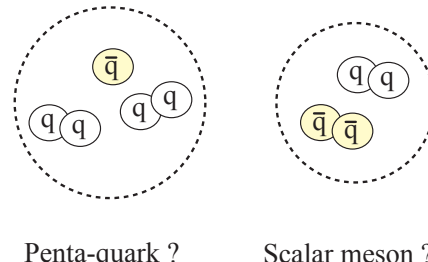


FIG. 1: Possible diquark contributions to the penta-quark and scalar meson.

## II. SCALAR MESONS

The objective of SCALAR collaboration is to understand scalar mesons in the framework of QCD. The confidence level of the sigma meson has been increasing, and an other scalar meson [8, 9],  $\kappa$ , has been reported by several experimental groups. In the modern hadron physics based on QCD, the chiral symmetry is an important ingredient and the sigma meson plays an essential role in it together with the pion.

The existence of the sigma meson was obscure for many years. The re-analyses of the  $\pi - \pi$  scattering phase shift have suggested a pole of the  $\sigma$  meson with  $I = 0$  and  $J^{PC} = 0^{++}$ [10]. In this analysis, the chiral symmetry, analyticity, unitarity and crossing symmetry are taken into account. Contributions of the  $\sigma$  pole were observed in the decay processes such as  $D \rightarrow \pi\pi\pi$ [11] and  $\Upsilon(3S) \rightarrow \Upsilon\pi\pi$  [12]. In 1996 PDG(Particle Data Group), “ $f_0(400-1200)$  or  $\sigma$ ” appeared below 1 GeV mass region, and “ $f_0(600)$  or  $\sigma$ ” in the 2002.

If the sigma meson exists, it is natural to consider the  $\kappa$  meson as a member of the nonet scalar states of chiral

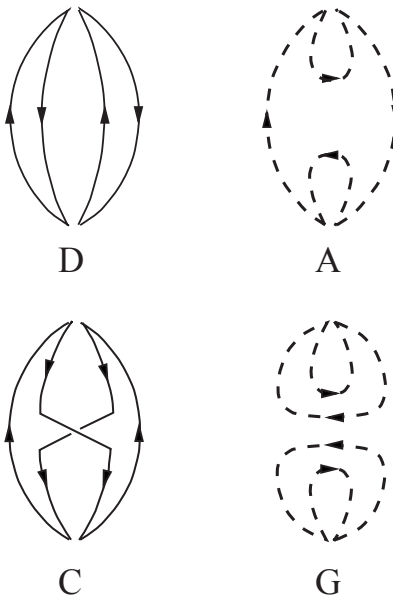


FIG. 2: The four types of quark line contraction that contribute to the pseudoscalar-pseudoscalar correlation function. Alford and Jaffe study diagrams D and C. [7]

$SU(3) \otimes SU(3)$  symmetry. Recently, the  $\kappa$  with  $I = 1/2$  is reported with mass  $m_\kappa \sim 800$  MeV [13, 14].

In order to establish the scalar meson spectroscopy as a sound and important piece of hadron physics, it is very important now to investigate these scalar mesons by lattice QCD. Lattice QCD provides a first-principle approach of hadron physics, and allows us to study non-perturbative aspects of quark-gluon dynamics. It is a relativistic formulation, and quarks are described as Dirac fermions. It is *not* a model, and apart from numerical limitations, there are no approximations. It is not a bound state calculation: neither a potential model nor Bethe-Salpeter calculation.

Lattice QCD is usually formulated in the Euclidean path integral as

$$Z = \int \mathcal{D}U \bar{\psi} \mathcal{D}\psi e^{-S_G - \bar{\psi} D\psi} = \int \mathcal{D}U \det D e^{-S_G}, \quad (2)$$

where  $S_G$  is the gluon kinetic action, whose continuum limit is  $-\int d^4x \text{Tr} F_{\mu\nu}^2 / 4$ . We construct a state with a definite quantum number and measure the decay in the channel,

$$\begin{aligned} G(x, y) &= \frac{1}{Z} \int \mathcal{D}U \bar{\psi} \mathcal{D}\psi H(y) H(x)^\dagger e^{-S_G - \bar{\psi} D\psi} \\ &= \langle H(y) H(x)^\dagger \rangle \rightarrow e^{-m|x-y|} \end{aligned} \quad (3)$$

where  $H(x)$  is a hadron operator. For scalar mesons,

$$H(x) = \sum_a \sum_\nu \sum_{f_1, f_2} C_{f_1 f_2} \bar{\psi}_\nu^{af_1} \psi_\nu^{af_2}. \quad (4)$$

The indices  $a, f_i$  and  $\nu$  stand for color, flavor and Dirac indices, respectively.  $H(x)^\dagger |0\rangle$  is a state whose quantum number is specified by the operator  $H$ .

$\pi$  mesons in the current lattice simulations are not sufficiently light and our sigma meson cannot decay into  $2\pi$ , *i.e.*, its width is zero. Any other particle, *e.g.*  $\rho$ ,  $\Delta$  and  $N^*$ , also have zero width in lattice QCD calculations in the literature. In the case of the sigma meson, this flaw should be kept in mind, since the two-pion component may be important.

There have been several attempts at lattice study of sigma mesons. To our knowledge, the first such calculation was carried out by deTar and Kogut [15], where the so-called disconnected diagram, or the OZI forbidden type diagram is discarded. The channel was called ‘valence’ sigma,  $\sigma_V$ . They measured the screening masses and observed that  $\sigma_V$  is much heavier than the  $\pi$  meson at the zero temperature, while  $\sigma_V$  and  $\pi$  degenerate as the temperature increases over  $T_c$ . Kim and Ohta calculated the valence sigma mass with staggered fermions for the lattice spacing  $a = 0.054$  fm and lattice size  $48a = 2.6$  fm [16]. They obtained  $m_\sigma/m_\pi = 1.4 \sim 1.6$  by varying  $m_\pi/m_\rho = 0.65 \sim 0.3$ .

Lee and Weingarten [17] have stressed the importance of the mixing the scalar meson and glueballs and concluded that  $f_0(1710)$  is the lightest scalar glueball dominant particle, while  $f_0(1390)$  is composed of mainly the  $u$  and  $d$  quarkonium. As discussed in the introduction, Alford and Jaffe analyzed the possibility that the sigma particle is an exotic state, *i.e.*,  $qq\bar{q}\bar{q}$  by a lattice QCD calculation [7].

All these calculations are in the quench approximation, *i.e.*, the fermion determinant in Eq.(2) is dropped, which corresponds to ignoring quark pair creation and annihilation diagrams. McNeile and Michael observed that the  $\sigma$  meson masses in the quench approximation and in the full QCD simulation are very different [18]. They also considered the mixing with the glueballs. They obtained a very small sigma meson mass, even smaller than the  $\pi$  mass, in the full QCD case.

There are two ongoing projects of  $\sigma$  meson spectroscopy : Riken-Brookhaven-Columbia (RBC) collaboration [19] and Scalar collaboration [20, 21]. The two approaches are complementary. The RBC collaboration employs the domain wall fermions, which respect the chiral symmetry, but include a quench approximation, while Scalar collaboration uses Wilson fermions, which break the chiral symmetry at a finite lattice spacing, but performs the full QCD simulation. RBC reported their simulation at  $a^{-1} = 1.3$  GeV on a  $16^3 \times 32$  lattice. They remedied the quench defect with the help of the chiral perturbation. They observed that the masses of the non-isosinglet scalar ( $a_0$ ) and the singlet scalar ( $\sigma$ ) are almost degenerate when the quark mass is heavy (above  $s$  quark mass regions), and that as the quark mass decreases, the  $a_0$  mass remains almost constant, but the mass of the  $\sigma$  decreases.

### A. Propagators of Sigma meson

The quantum numbers of the  $\sigma$  meson are  $I = 0$  and  $J^{PC} = 0^{++}$ ; we adopt the  $\sigma$  meson operator of

$$\hat{\sigma}(x) \equiv \frac{\bar{u}(x)u(x) + \bar{d}(x)d(x)}{\sqrt{2}}, \quad (5)$$

where  $u$  and  $d$  indicate corresponding quark spinors, and we suppress the color and Dirac indices. The  $\sigma$  meson propagator is written as

$$\begin{aligned} G_\sigma(y, x) &= \langle T\hat{\sigma}(y)\hat{\sigma}(x)^\dagger \rangle \\ &= \frac{1}{Z} \int \mathcal{D}U \mathcal{D}\bar{u} \mathcal{D}u \mathcal{D}\bar{d} \mathcal{D}d \frac{\bar{u}(y)u(y) + \bar{d}(y)d(y)}{\sqrt{2}} \\ &\times \left( \frac{\bar{u}(x)u(x) + \bar{d}(x)d(x)}{\sqrt{2}} \right)^\dagger \\ &\times e^{-S_G - \bar{u}Du - \bar{d}Dd}. \end{aligned} \quad (6)$$

By integrating over  $u$ ,  $\bar{u}$ ,  $d$  and  $\bar{d}$  fields, the  $\sigma$  meson propagator leads to

$$\begin{aligned} G_\sigma(y, x) &= -\langle \text{Tr}D^{-1}(x, y)D^{-1}(y, x) \rangle \\ &+ 2\langle \text{Tr}D^{-1}(y, y)\text{Tr}D^{-1}(x, x) \rangle \\ &- 2\langle \text{Tr}D^{-1}(y, y) \rangle \langle \text{Tr}D^{-1}(x, x) \rangle \\ &= -\langle \text{Tr}D^{-1}(x, y)D^{-1}(y, x) \rangle \\ &+ 2\langle (\sigma(y) - \langle \sigma(y) \rangle)(\sigma(x) - \langle \sigma(x) \rangle) \rangle \end{aligned} \quad (7)$$

where  $\sigma(x) \equiv \text{Tr}D^{-1}(x, x)$ . “Tr” represents a summation over color and Dirac spinor indices. In Eq.(7),  $D^{-1}$ ’s are  $u$  and  $d$  quark propagators. Here we assumed that the  $u$  and  $d$  quark propagators are equivalent because  $u$  and  $d$  quark masses are almost the same.

From Eq.(7), we see that the  $\sigma$  propagator consists of two terms. The first term corresponds to the connected diagram, *i.e.*, a  $\bar{q}q$ -type meson which is the first term in Fig.3. The second term is the “disconnected” diagram; it is the correlation of  $\sigma(x) = \text{Tr}D^{-1}(x, x)$  at two points  $x$  and  $y$  corresponding to the second term in Fig.3. The term “disconnected” is not appropriate since the corresponding matrix element is, of course, not factorized; quark lines are connected by gluon interactions. Nevertheless, we use this jargon in the following.

The quantum number of the  $\sigma$  meson ( $I = 0$  and  $J^P = 0^+$ ) is the same as that of the vacuum, and the vacuum expectation value of the  $\sigma$  operator,  $\langle \sigma(x) \rangle$ , does not vanish. Therefore, the contribution of  $\langle \sigma(x) \rangle$  should be subtracted from the  $\sigma$  operator. See Eq.(7).

Note that since the full QCD simulation includes the  $q - \bar{q}$  pair creation/annihilation, not only the first two diagrams in Fig.3 but also  $\bar{q}q\bar{q}q$ ,  $\bar{q}q\bar{q}q\bar{q}q$ ,  $\dots$  appear at intermediate states.

For  $\kappa^+$ , the operator is  $H(x) = \sum_a \sum_\nu \bar{s}_\nu^a u_\nu^a$ , and we have only the connected diagram,

$$G_\kappa(y, x) = -\langle \text{Tr}D_s^{-1}(x, y)D^{-1}(y, x) \rangle, \quad (8)$$

where  $D_s^{-1}$  is the  $s$  quark propagator.

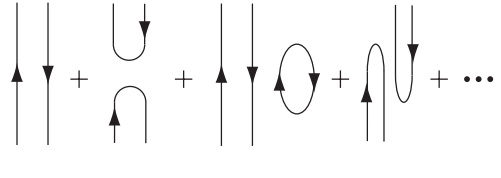


FIG. 3: Quark diagrams for the scalar meson,  $\sigma$ , in lattice simulations of full QCD.

### B. Numerical simulations

In this project, we use only standard well-established techniques for numerical calculations, and want to see the outcome. We employ Wilson fermions and the plaquette gauge action. Full QCD simulations were done by the Hybrid Monte Carlo (HMC) algorithm.

CP-PACS performed a very large-scale simulation of light meson spectroscopy in the full QCD calculation [22]. We use here the same values of the simulation parameters, *i.e.*,  $\beta = 4.8$  and  $\kappa = 0.1846, 0.1874, 0.1891$ , except lattice size; our lattice,  $8^3 \times 16$ , is smaller. We employ the point source and sink; smaller lattice size leads to larger mass due to a higher state mixture,  $G_\sigma = C \exp(-mt) + C' \exp(-m't) + \dots$ . In the point source/sink case,  $C, C', \dots$  are positive. In other words, our mass values on the small size lattice should be considered as the upper limit. We have checked that the values of  $m_\pi$  and  $m_\rho$  are consistent with those of CP-PACS.

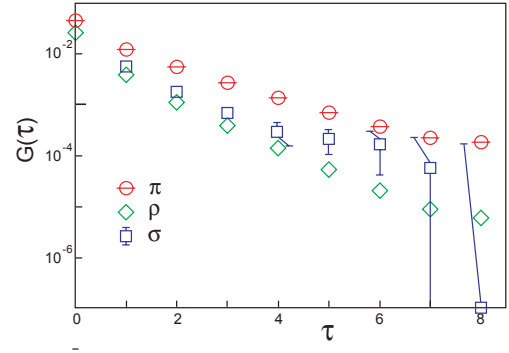


FIG. 4: Propagators of  $\pi$ ,  $\rho$  and  $\sigma$  for  $\kappa = 0.1891$ .

It is very difficult to evaluate the disconnected part of the propagator, since we must calculate  $\text{Tr}D^{-1}(x, x)$  for all lattice sites  $x$ . We used the  $Z_2$  noise method to calculate the disconnected diagrams and the subtraction terms of the vacuum  $\langle \sigma \rangle$ . Each of these terms is of the order of ten, and  $\langle (\sigma - \langle \sigma \rangle)(\sigma - \langle \sigma \rangle) \rangle$  becomes less than  $10^{-4}$ , as shown in Fig.5. Therefore, high accuracy is required for the calculation. One thousand random  $Z_2$  numbers are generated. Our numerical results show that the values of the first and the second terms in Eq.(7) are of the same

order. Therefore, in order to obtain the signal correctly as the difference between these terms, high-precision numerical simulations and careful analyses are required. We have investigated the relationship between the amount of  $Z_2$  noise and the achieved accuracy in Ref.[20]. Gauge configurations were created by HMC in the SX5 vector supercomputer, and most disconnected propagator calculations by the  $Z_2$  noise method were mainly performed on the SR8000 parallel machine at KEK.

The propagators of  $\pi$ ,  $\rho$  and  $\sigma$  for  $\kappa = 0.1891$  are shown in Fig.4. The connected and disconnected parts of the  $\sigma$  propagator are shown in Fig.5. It is difficult to obtain  $\sigma$  propagator at large  $\tau$  since the precision of our calculation is limited to  $O(G(\tau)) \sim 10^{-4}$ .

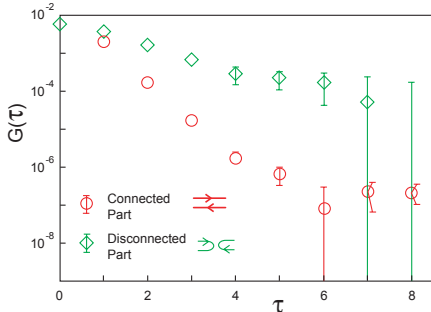


FIG. 5: Propagators of the connected and disconnected diagram of  $\sigma$  for  $\kappa = 0.1891$ .

From our results, we evaluate the critical value of the hopping parameter  $\kappa_c = 0.195(3)$  and lattice space  $a = 0.207(9)$  fm (CP-PACS has obtained  $\kappa_c = 0.19286(14)$  and  $a = 0.197(2)$  fm). Figure 6 (left) shows masses of  $\rho$ ,  $\sigma$  and  $\pi$  as functions of  $1/\kappa$ . We find that  $m_\sigma/m_\rho$  at the chiral limit is  $0.33 \pm 0.09$ . Our results indicate the existence of a light  $\sigma$  in the region  $m_\pi < m_\sigma \leq m_\rho$ .

Finally, we present our preliminary result for  $\kappa$  meson using the same common configurations. The  $s$  quark is treated as a valence, *i.e.*, is used only in the propagator (8), not as a sea quark. We adopt the same hopping parameter values,  $\kappa = 0.1846, 0.1874$  and  $0.1891$  for  $u$  and  $d$  quarks. We calculate three values of the hopping parameter for the  $s$  quark:  $\kappa_s = 0.1835, 0.1840$  and  $0.1845$ . For each  $\kappa_s$ , we calculate masses of  $\kappa$ ,  $K^*$  and  $K$  mesons, and extrapolate them to the chiral limit. Then we tune the  $s$  quark hopping parameter,  $\kappa_s$ , to give the best experimental values for  $m_{K^*}$  and  $m_K$ . Figure 6 (right) shows  $m_\kappa a$ ,  $m_{K^*} a$  and  $m_K a$  as functions of  $1/\kappa$  for  $\kappa_s = 0.1840$ . Our preliminary analysis shows that value of  $m_\kappa/m_{K^*}$  at the chiral limit is around 2.0.

An interesting observation is that the disconnected part gives a significant contribution, and this diagram makes the  $\sigma$  meson light. This cannot be accessed in the framework of the non-relativistic quark model. This point should be kept in mind in future phenomenological analyses of the sigma meson, and also in lattice studies. Note that the  $\kappa$  meson does not have such a mechanism,

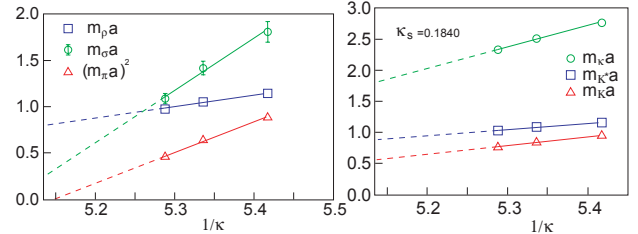


FIG. 6: Left :  $m_\rho$ ,  $m_\sigma$  and  $(m_\pi)^2$  in the lattice unit as functions of the inverse hopping parameter. Right :  $m_\kappa$ ,  $m_{K^*}$  and  $m_K$  in the lattice unit as functions of the inverse hopping parameter. The  $s$  quark hopping parameter is  $\kappa_s = 0.1840$ .

and therefore these two scalar meson masses can be different. The  $\kappa$  and the valence  $\sigma$  (connected part) have the same structure in their propagators, but  $s$  quark mass is heavier than those of  $u$  and  $d$ . Therefore  $m_\kappa > m_{conn}$ , where  $m_{conn}$  is a mass corresponding to the connected part,  $\sigma V$ .

The calculations reported here have limitations: masses of  $u$  and  $d$  quarks are not light enough, simulations are done at a strong coupling region and the accuracy of the disconnected part is not sufficient. These defects will, however, be gradually overcome. In lattice calculation, once someone establishes the scale of simulation required to obtain meaningful results, many improved and large-scale works succeed. Therefore in a few years, the lattice study of scalar mesons will provide important and fundamental information to deepen our understanding of hadron physics.

### III. POTENTIAL IN DIQUARK SYSTEM

The penta-quark state ( $\Theta^+$ ) may be a bound state of  $(ud)(ud)\bar{s}$ , where  $(ud)$  stands for highly correlated  $u$  and  $d$  quark pairs.[6] See Prof. Jaffe's paper in the proceedings. At high baryon number density and low temperature, a family of color superconducting phases is expected to occur, due to the quark pairing driven by the BCS mechanism.[2] See Ref.[3] for a review of the history of diquarks and their roles in high energy reactions.

As far as we know, there has been no literature to investigate the quark-quark potential using lattice QCD which provides us a non-perturbative and first principle base to study diquark system. There has been only one study by Wetzorke and her collaborators, where diquark correlation functions were calculated in lattice QCD [23].

#### A. Heavy quark-quark system on a lattice

In this paper, we study the heavy quark-quark free energies at finite temperature which are obtained from the Polyakov line correlation (PLC). PLC was first discussed

by McLerran and Svetitsky[24]. The free energy  $F$  is given by

$$e^{-\beta F} = \sum_{\phi} \langle \phi | e^{-\beta H} | \phi \rangle, \quad (9)$$

where  $|\phi\rangle$  is a state of gluons and heavy quarks. For a heavy quark-quark system of the color anti-triplet,

$$|\phi\rangle = \epsilon_{abc} \psi^b(\vec{x}_1, t=0)^\dagger \psi^c(\vec{x}_2, t=0)^\dagger |Gluons\rangle \quad (10)$$

Here  $a, b$  and  $c$  are the color indices. Now, the summation in Eq.(9) is taken over  $a$  and all gluonic states. Using the following relations[24],

$$\psi(\vec{x}, t) = L\psi(\vec{x}, 0), \quad (11)$$

$$\{\psi^a(\vec{x}, t=0), \psi^b(\vec{y}, t=0)^\dagger\} = \delta_{a,b} \delta_{\vec{x}, \vec{y}}, \quad (12)$$

where

$$L(\vec{x}) = \prod_{t=1}^{N_t} U_4(\vec{x}, t), \quad (13)$$

and

$$\epsilon_{abc} \epsilon_{ab'c'} = \delta_{b,b'} \delta_{c,c'} - \delta_{b,c'} \delta_{c,b'}, \quad (14)$$

we obtain the free energies for  $qq$  sector in the symmetric and anti-symmetric channels,

$$\begin{aligned} \exp(-\beta F_s(R)) &= \frac{3}{4} \langle \text{Tr}L(\vec{x}_1) \text{Tr}L(\vec{x}_2) \rangle + \frac{3}{4} \langle \text{Tr}L(\vec{x}_1) L(\vec{x}_2) \rangle \\ &= \boxed{\square}, \\ \exp(-\beta F_{as}(R)) &= \frac{3}{2} \langle \text{Tr}L(\vec{x}_1) \text{Tr}L(\vec{x}_2) \rangle - \frac{3}{2} \langle \text{Tr}L(\vec{x}_1) L(\vec{x}_2) \rangle \\ &= \boxed{\square} \end{aligned} \quad (15)$$

where  $F_{s(as)}$  are the difference of the free energy with and without the static color symmetric (anti-symmetric) quarks located at  $\vec{x}_1$  and  $\vec{x}_2$ ,  $R = |\vec{x}_1 - \vec{x}_2|$  and  $\beta = 1/T$ .

The formula (15) is gauge dependent, and therefore we need the gauge fixing. We employ the stochastic gauge fixing quantization (SGFQ) with the Lorentz-type gauge fixing proposed by Zwanziger[25]:

$$\frac{dA_\mu^a}{d\tau} = -\frac{\delta S}{\delta A_\mu^a} + \frac{1}{\alpha} D_\mu^{ab}(A) \partial_\nu A_\nu^b + \eta_\mu^a, \quad (16)$$

where  $\alpha$ ,  $D_\mu^{ab}$  and  $\eta_\mu^a$  correspond to a gauge parameter, a covariant derivative and Gaussian random noise, respectively. The lattice formulation and a more detailed explanation of this algorithm can be found in Refs. [26–28].

In the quenched approximation, the system has  $Z_3$  symmetry. The gauge action is invariant under the transformation,  $U_4(x) \rightarrow zU_4(x)$  or  $z^2U_4(x)$  on a time-slice hyperplane, where  $z = \exp(2\pi i/3)$ . In this transformation, both  $\text{Tr}L(\vec{x}_1)\text{Tr}L(\vec{x}_2)$  and  $\text{Tr}L(\vec{x}_1)L(\vec{x}_2)$  get a factor  $z^2$  or  $z^4$ . After infinite sweeps, Eqs.(15) vanishes since  $1 + z^2 + z^4 = 0$ . Therefore we restrict our simulations in the region  $-\pi/3 < \text{Phase } L < \pi/3$ .

## B. Numerical results

In order to calculate the color dependent Polyakov correlation functions at finite temperature, we perform the quenched  $SU(3)$  lattice simulation with the standard plaquette action. Simulation parameters are the same as in our previous study for the measurement of  $q\bar{q}$  PLC functions in the QGP phase[29]. The spatial lattice volume is  $24^3$  and the temporal lattice size is set as  $N_t = 6$ , which determines the temperature as  $T = 1/N_t a$ , where  $a$  is a lattice spacing. The corresponding critical temperature is estimated as  $T_c \sim 256\text{MeV}$  in Ref.[30]. The system temperature is changed when we vary the lattice cut-off which is determined by Monte Carlo renormalization group analysis [31]. All of the PLCs are measured every ten Langevin steps and normalized by the value  $\langle \text{Tr}L(0) \rangle^2$ . The amount of statistics is from 3000 to 10000 after approximately 3000 steps are discarded as thermalization.

The typical behaviors of the symmetric and anti-symmetric free energy at  $T/T_c = 2.02, 3.04, 5.61$  are shown in Fig. 7. The symmetric channel gives the repulsive force, while the anti-symmetric one the attractive force. As the system temperature is varied, each potential is changed and their variations are small.

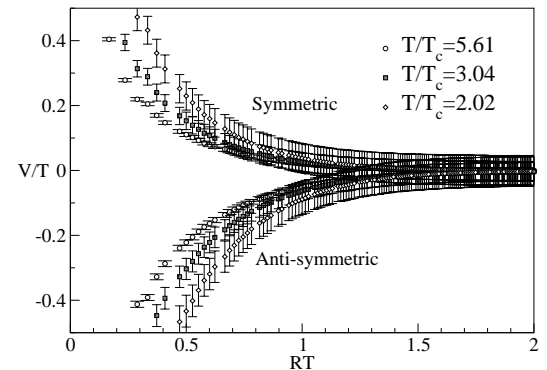


FIG. 7: The behavior of  $qq$  free energy in symmetric and anti-symmetric channel at Langevin step width  $\Delta\tau = 0.03$ .

In order to investigate the temperature dependence of these free energies in more detail, we define an effective force as

$$\frac{f(R, T)}{T^2} = -\frac{1}{T^2} (F(R+1) - F(R)). \quad (17)$$

The temperature dependence of the effective force strength is shown in Fig. 8. As the temperature increases, the effective force strength in both channels decreases.

In the leading order perturbation (LOP), coefficient of the color exchange terms in the symmetric and anti-symmetric channels are  $C_{qq}[6] = +\frac{1}{3}$  and  $C_{qq}[3^*] = -\frac{2}{3}$ .

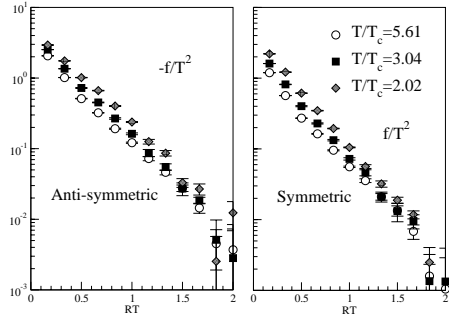


FIG. 8: The temperature dependence of the effective force in symmetric and anti-symmetric channels at Langevin step width  $\Delta\tau = 0.03$ .

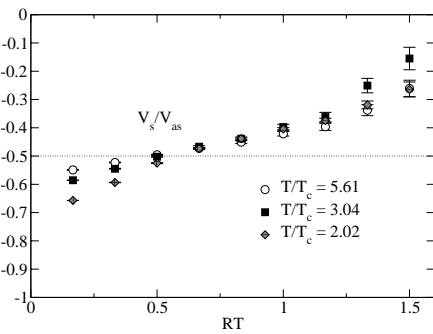


FIG. 9: The temperature dependence of the ratio  $V_s/V_{as}$  at Langevin step width  $\Delta\tau = 0.03$ . The dash-dot line stands for the expected ratio,  $C_{qq}[6]/C_{qq}[3^*] = -0.5$  at short distances.

We compare the force strength in symmetric and anti-symmetric channel and define the ratio,  $F_s/F_{as}$ , which approaches the value  $C_{qq}[6]/C_{qq}[3^*] = -0.5$  at short distances. Fig.9 shows the ratios at  $T/T_c = 2.02, 3.04, 5.61$ . As the temperature increases the ratios at short distances are comparable with the expected values; however, as the temperature decreases, it deviates from  $-0.5$ .

We here check the  $\Delta\tau$  dependence. In Fig. 10,  $V_s$  and  $V_{as}$  are shown for several values of  $\Delta\tau$ . They depend little on  $\Delta\tau = 0.0125 \sim 0.03$ .

Two gauge dependent channels,  $qq$  symmetric and anti-symmetric, are well controlled in the framework of the stochastic quantization with Lorentz type gauge fixing term. As a result we find that the anti-symmetric free energy indicates the attractive force while the symmetric one the repulsive force.

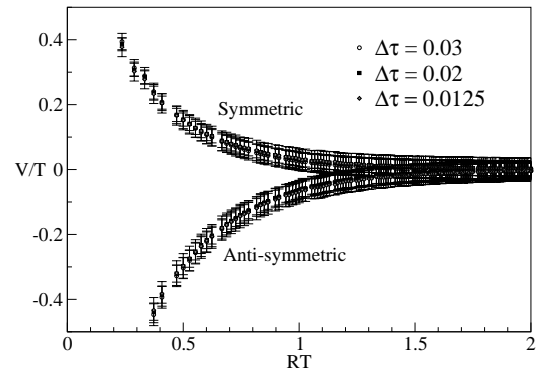


FIG. 10: Langevin step width  $\Delta\tau$  dependence of singlet and octet potentials at  $T/T_c = 3.04$ .

### C. Diquark force at zero-temperature

Data presented here are very encouraging. By fixing the gauge, we can investigate the quark-quark potential. It is very interesting if we can extend the analysis to zero temperature. An obstacle is that we measure here the correlation between the Polyakov loops, which vanish at zero temperature. Wilson loops are not proper for studying  $qq$  potential.

An interesting operator was proposed in Ref.[32], which is correlations of finite length Polyakov loops:

$$G_n^{q\bar{q}}(R) = \langle L(\vec{x}_1, t; n) L(\vec{x}_2, t; n)^\dagger \rangle, \quad (18)$$

where  $R \equiv |\vec{x}_1 - \vec{x}_2|$ , and

$$L(\vec{x}, t; n) \equiv U_4(\vec{x}, t) U_4(\vec{x}, t+1) \cdots U_4(\vec{x}, t+n). \quad (19)$$

In the Coulomb gauge, the operator  $L(\vec{x}, t; n)$  has the following remnant gauge symmetry in time slices,

$$L(\vec{x}, t; n) \rightarrow \omega(t)^\dagger L(\vec{x}, t; n) \omega(t+n) \quad (20)$$

Once we carry out the Coulomb gauge fixing, the correlation, (18), is similar to the Wilson loop, and it behaves as

$$G_n^{q\bar{q}}(R) \sim e^{-\sigma^2 R n}, \quad (21)$$

in the confinement phase, where  $\sigma$  is the string tension. We extend this operator to the di-quark system.

$$G_n^{q\bar{q}}(R) = \langle L(\vec{x}_1, t; n) L(\vec{x}_2, t; n) \rangle. \quad (22)$$

This  $qq$  correlation vanishes due to the remnant symmetry (20). Therefore we further a temporal gauge fixing in the Coulomb gauge, which can be realized by maximizing

$$\sum Re Tr U_4(\vec{x}, t). \quad (23)$$

Under the transformation,  $U_4(x) \rightarrow z U_4(x)$  or  $z^2 U_4(x)$ , on a time-slice hyperplane between  $t$  and  $t+n$ ,

$L(\vec{x}_1, t; n)L(\vec{x}_2, t; n)$  get a factor  $z^2$  or  $z^4$ . Therefore after infinite sweeps, Eq.(22) vanishes and we should restrict our simulations in the region  $-\pi/3 < \text{Phase } L < \pi/3$ .

Based on the formula, we are now preparing the calculation of  $G_n^{qq}(R)$  to study the diquark force in the confinement phase.

- 
- [1] LEPS Collaboration: T. Nakano, et al., Phys.Rev.Lett. **91** (2003) 012002 (hep-ex/0301020).
  - [2] M. G. Alford, Ann. Rev. Nucl. Part. Sci. **51** (2001) 131, hep-ph/0102047.
  - [3] M. Anselmino, E. Predazzi, S. Ekelin, S. Fredriksson, and D.B. Lichtenberg, Rev. Mod. Phys. **65** (1993) 1199.
  - [4] De Rujula, H. Georgi, and S. L. Glashow, Phys. Rev. D **12**, 147 (1975).
  - [5] E. V. Shuryak and J. L. Rosner, Phys. Lett. B **218**, 72 (1989).
  - [6] R. L. Jaffe and F. Wilczek, Phys. Rev. Lett. **91** (2003) 232003, hep-ph/0307341.
  - [7] M. Alford and R. L. Jaffe, Nucl. Phys. B578 (2000) 367-382, (hep-lat/0001023); See also, M. Alford and R. L. Jaffe, hep-lat/0306037, “Scalar Mesons as  $q\bar{q}$   $q^2$ ? Insight from the Lattice”.
  - [8] Possible existence of the sigma-meson and its implications to hadron physics, KEK Proceedings 2000-4, So-ryushiron Kenkyu (kyoto) 102 (2001) E1; The proceedings of this workshop.
  - [9] F. E. Close and N. A. Törnqvist, J. Phys. G: Nucl. Part. Phys. **28** (2002) R249.
  - [10] K. Igi and K.-I. Hikasa, Phys. Rev. D**59**, 034005 (1999).
  - [11] E. M. Aitala *et al*, Phys. Rev. Lett. **86** (2001) 770.
  - [12] M. Ishida *et al.*, Phys. Lett. B518 (2001) 47-54.
  - [13] B791 collaboration, Phys. Rev. Lett. **89** (2002) 121791, hep-ex/0204018.
  - [14] J.Z. Bai, et al, BES collaboration, hep-ex/0304001.
  - [15] C. DeTar and J. B. Kogut, Phys. Rev. D**36** (1987) 2828.
  - [16] S. Kim and S. Ohta, Nucl. Phys. Proc.Suppl. **53** (1997) 199 (hep-lat/9609023), *ibid.* **63** (1998) 185 (hep-lat/9712014).
  - [17] W. Lee and D. Weingarten, Phys. Rev. D**61** (1999) 014015.
  - [18] C. McNeile and C. Michael, Phys. Rev. D**63** (2001) 114503.
  - [19] S. Prelovsek and K. Orginos, hep-lat/0209132.
  - [20] SCALAR Collaboration, Nucl. Phys. Proc. Suppl. **106** (2002) 272.
  - [21] SCALAR Collaboration, hep-lat/0210012
  - [22] S. Aoki *et al.*, Phys. Rev. D**60** (1999) 114508.
  - [23] I. Wetzorke and F. Karsch, hep-lat/0008008; M. Hess, F. Karsch, E. Laermann and I. Wetzorke, Phys.Rev. D**58** (1998) 111502 (hep-lat/9804023).
  - [24] L. D. McLerran and B. Svetitsky, Phys. Rev. D **24** (1981), 450.
  - [25] D. Zwanziger, Nucl. Phys. **B192**, 259 (1981).
  - [26] A. Nakamura and M. Mizutani, *Vistas in Astronomy* (Pergamon Press), vol. **37**, 305 (1993); M. Mizutani and A. Nakamura, Nucl. Phys. B(Proc. Suppl.) **34**, 253 (1994); A. Nakamura, Prog. Theor. Phys. Suppl. No. **131**, 585, 1998.
  - [27] A. Nakamura, I. Pushkina, T. Saito and S. Sakai, Phys. Lett. B **549**, 133 (2002).
  - [28] A. Nakamura, T. Saito and S. Sakai, Phys. Rev. D **69**, 014506 (2004).
  - [29] A. Nakamura and T. Saito, to be submitted to PTP.
  - [30] G. Boyd, J. Engels, F. Karsch, E. Laermann, C. Lege-land, M. Lütgemeier, and B. Petersson, Phys. Rev. Lett. **75**, 4169 (1995); Nucl. Phys. B **469**, 419 (1996).
  - [31] QCDSF collaboration, K. Akemi, et al., Phys. Rev. Lett. **71**, 3063 (1993).
  - [32] E. Marinari, M. L. Paciello, G. Parisi and B. Taglienti, Phys. Lett. B298 (1993) 400.